ISSN 2712-0554
Heritage and Sustainable Development *Original Research*
Vol. 6, No. 2, July 2024, pp.429-444
https://doi.org/10.37868/hsd.v6i2.583

River morphological behavior between two barrages on the Euphrates: A case study

Zainab Dekan Abbass [1*], Jaafar S. Maatooq[2], Mustafa M. Al-Mukhtar[3]
[1,2,3] Civil Engineering Department, University of Technology, Baghdad, Iraq
[1]Department of Environmental Planning, University of Kufa, Kufa, Iraq

*Corresponding author E-mail: bce.19.83@grad.uotechnology.edu.iq

Received May 7, 2024
Revised Jun. 13, 2024
Accepted, Jun. 19, 2024

Abstract

The Abbassia-Shammia stream is a meandering reach in Najaf Province downstream of the Euphrates. The geomorphological traits and process-based assessment of large rivers are rarely observed globally, particularly in less developed nations. The need for such evaluation arose due to climate change, hydraulic structure construction, and the possibility of extreme droughts and floods. The hydraulic and morphological properties of the Abbassia-Shammia reach were significantly altered owing to the installation of successive barrages and climatic change. This paper aims to assess the river morphological behavior downstream of the Euphrates near the Abbassia-Shammia reach for 32 km length through the bed change investigation process, i.e. river sedimentation and erosion. The morphological performance of the Euphrates reaches between two series of barrages, namely Abbassia and Shammia, was simulated using HEC RAS2D, a tool developed by the River Analysis System program of the Hydrologic Engineering Center. The research revealed that bed change levels ranged from 5.87 meters of sedimentation to 5.720 meters of erosion. Furthermore, the results showcased how effectively the HEC RAS2D model accurately captured the features of a Euphrates section between two barrages. The results of the study provide insights into the future behavior of channels. They can help to address the issues caused by the prevailing fluvial processes such as sedimentation and erosion.

Keywords: River sustainability, Hydraulic structures, Abbassia-Shammia, Morphology, Sediment transport capacity

1. Introduction

The impact of change made by hydraulic structures in particular on the geomorphology of rivers and human-made river systems generally, has been investigated since the commencement of the quick worldwide development of large reservoirs around the 1950s. The shape of natural river morphology is formed by the prolonged interplay of water, riverbed conditions, and sediment [1]. Over time, lateral or vertical changes may occur to river morphology. This occurrence requires a thorough understanding of the parameters causing these issues.

River morphological changes are mostly affected by variations in water flows and sediment loads [2], [3]. The classification of river morphology includes deterioration, aggradation, and broadening [4]. Due to the complicated flow pattern and unequal sediment distribution and concentration, most natural rivers have suspended sediment and bed-load sediment. Deposition and erosion connect these two stages, causing constant changes in suspension and riverbed granulometry. Solid particle exchange between the water and the river bed modifies bed morphology and perhaps bed composition [5].

Several authors, such as [6], and [7] have investigated the impact of granulometric composition on the process of sediment movement in the last decade. The upstream dam constructions had a large influence on the sediment reduction downstream of the Parma River in northern Italy, which resulted in morphological degradation [8], [9]. The researchers analyzed the morphological changes over time and annual cross-sectional data and water and sediment data from hydrological stations in Xianyang, Lintong, and Huaxian along the lower Weihe River [10]. The study period spanned from 2006 to 2018 and focused on the response of river cross-sections to fluctuations in water and sediment levels. The studies by [11], [12], and [13] have shown that frequent and intense flows have a substantial impact on the physical characteristics of big, braided gravel-bed rivers.

The Euphrates, a vital watercourse for the area, has undergone substantial hydrological modifications as a result of the combined impacts of climate change and upstream water management policies. The Abbassia-Shammia reach is the primary segment of the Euphrates, supplying water to the communities situated along its shores. The Euphrates is globally acknowledged as one of the most significant ancient rivers. The river is notable for being the longest in southwest Asia, with a length of 2786 km and a drainage basin of around 440,000 km2 [14]. Other areas of morphologic behavior still have not been extensively investigated.

The Abbassia reach, which extends for 32 kilometers from Abbassia city in Kufa to Al-Shamiya city in Dywania, has not undergone prior analysis of hydraulic and morphologic behaviors. The building of the Abbassia and Shammia barrages was started by the Iraqi Ministry of Water Resources (IMoWR) in 1982. The barrages are situated in the lower part of the Babylon governorate. Most of the literature on Abbassia-Shammia primarily examines the geometric properties and/or the composition of the bed material. The primary approach employed in this research involved a cross-sectional survey, along with laboratory analysis of bed materials and field surveys. These approaches were implemented in order to do analytical comparisons with global equations. [15], [16], and [17]. These studies only focus on fieldwork and laboratory work, neglecting the investigation of rivers' hydrodynamics. This work represents the initial endeavor to comprehend the reaching behavior by utilizing on-site data, with available data which includes the officially required data from [18], and the analysis was conducted using HECRAS2D Software.

Prior studies have predominantly concentrated on the one-dimensional aspects of the river, neglecting its lateral or vertical dimensions. The current study focuses on the flow and sediment characteristic effects on river morphology through a field study in the Abbassia-Shammia reach using HECRAS2D. The results of the study provide insights into the future behavior of channels. Thus, the study can help to address the issues caused by the prevailing fluvial processes.

1.1. Study area

The Abbassia-Shammia reach was chosen as the targeted study region. The Abbassia and Shammia barrages were built in 1982 on the Kifil-Shanafiyah branch of the Euphrates, located downstream in the Babylon governorate. Their primary aim is to facilitate irrigation. The primary purpose of the barrages is to control and oversee the water flow inside the Euphrates region. The specified flow rate of water passing through the barrages is 1000 cubic meters per second, while the water level downstream of the Abbassia barrage is measured at 23.8 meters. According to the operational report, the current operating discharge in the Abbassia barrage runs from 30 to 60 cubic meters per second, with a water level of 23.5 meters. Each barrage consists of six rectangular openings each measuring 12 m in width and 6 m in height, equipped with a steel radial gate. The research reach spans a distance of 32 kilometers, extending from the Abbassia barrage to the Shammia barrage. Figure 1 depicts

the precise position of the Al-Abbassia-Shammia barrier and the exact path of the river that is the subject of the study.

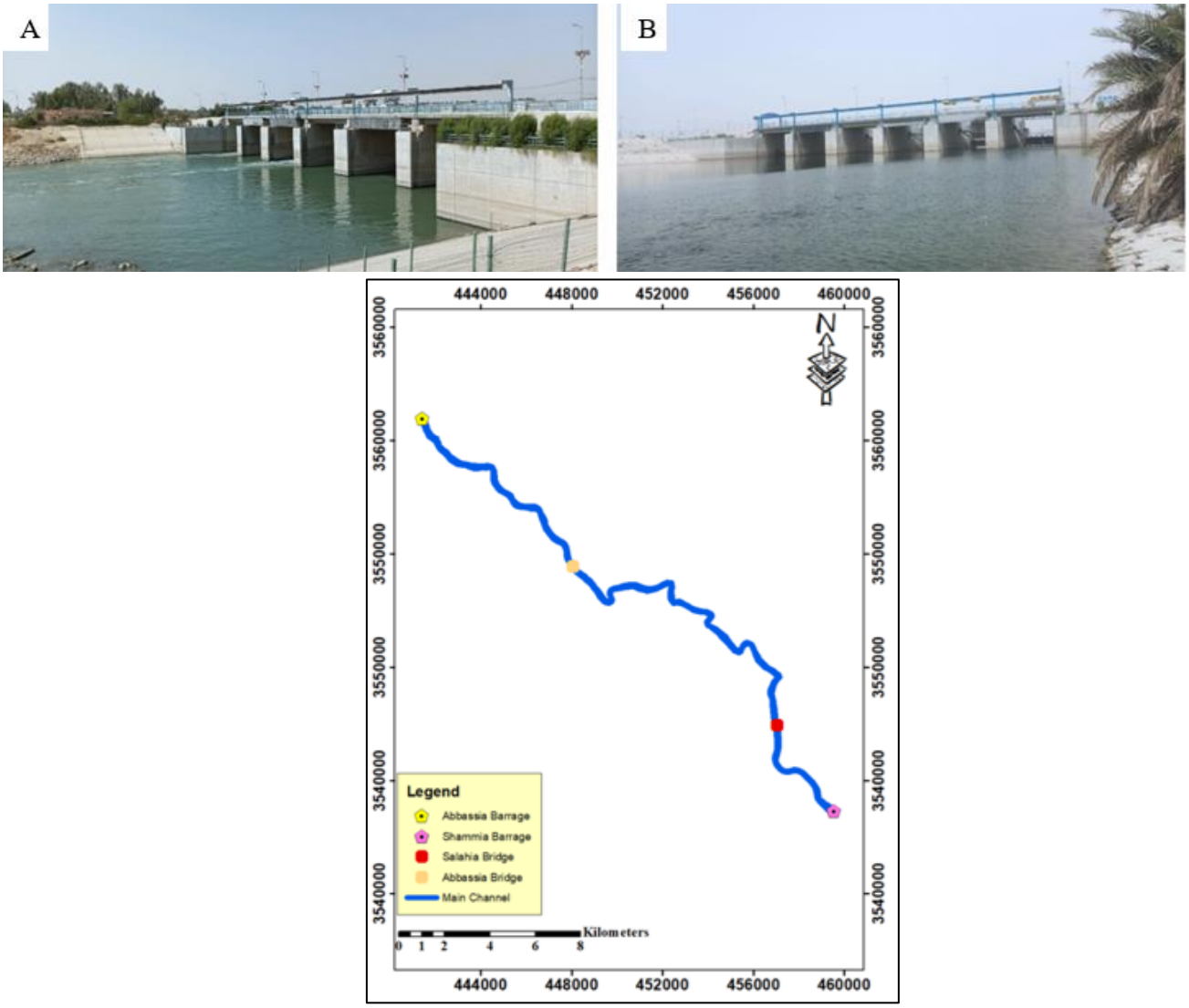

Figure 1. Study area location; A. Al-Abbassia barrage; B. Al-Shammia barrage

2. Materials and methods

2.1. Data collection

This work provides the results of the hydraulic model using the flow and stage hydrograph for the year 2023 (Figures 2 and 3), as documented by [18] for the Abbassia-Shammia River. It was used as a boundary condition in HECRAS2D. The objective of this section is to simulate the hydraulic and morphologic characteristics of the research area. A bathymetric survey was conducted using the Acoustic Doppler Current Profiler (ADCP) to measure water depth and discharge; cross-section profile details are shown in Figure 4. Furthermore, samples of suspended load and bed material were field investigated. An essential need for creating a hydraulic model is a series of cross-sections (XS) that span the whole channel. Historically, these models have been developed by systematically examining several cross-sections of the stream segment to be simulated. The authors collected the data for river cross-sections by field inquiry. The Abbassia-Shammia reach was surveyed in two sets of cross-sections. The first set consisted of four cross-sections surveyed until March 22, 2023. The second set consisted of six cross-sections surveyed until May 17, 2023. Both sets of cross-sections were employed in the simulation period. The recorded flow velocities ranged from 0.011 to 0.174 m/s, with the highest velocity seen at CS8 located downstream of Abbassia barrage, at a distance of 20 km. The positions of the 10 cross-sections are shown in Figure 5; Figure 6 displays many images captured during the field investigation.

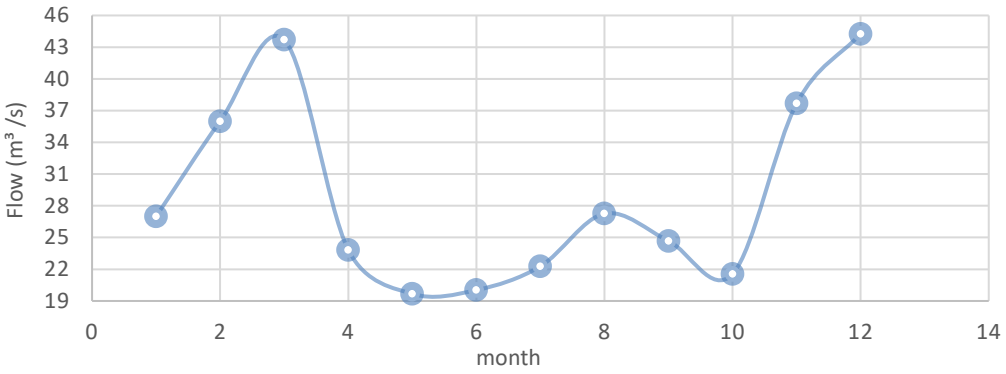

Figure 2. Flow hydrograph recorded upstream of Abbassia-Shammia reach in 2023 [18]

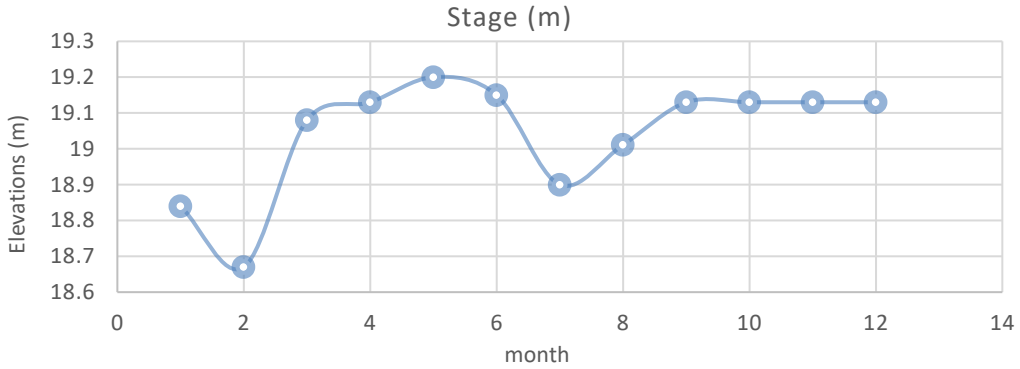

Figure 3. Stage hydrograph recorded downstream of Abbassia-Shammia reach in 2023 [18]

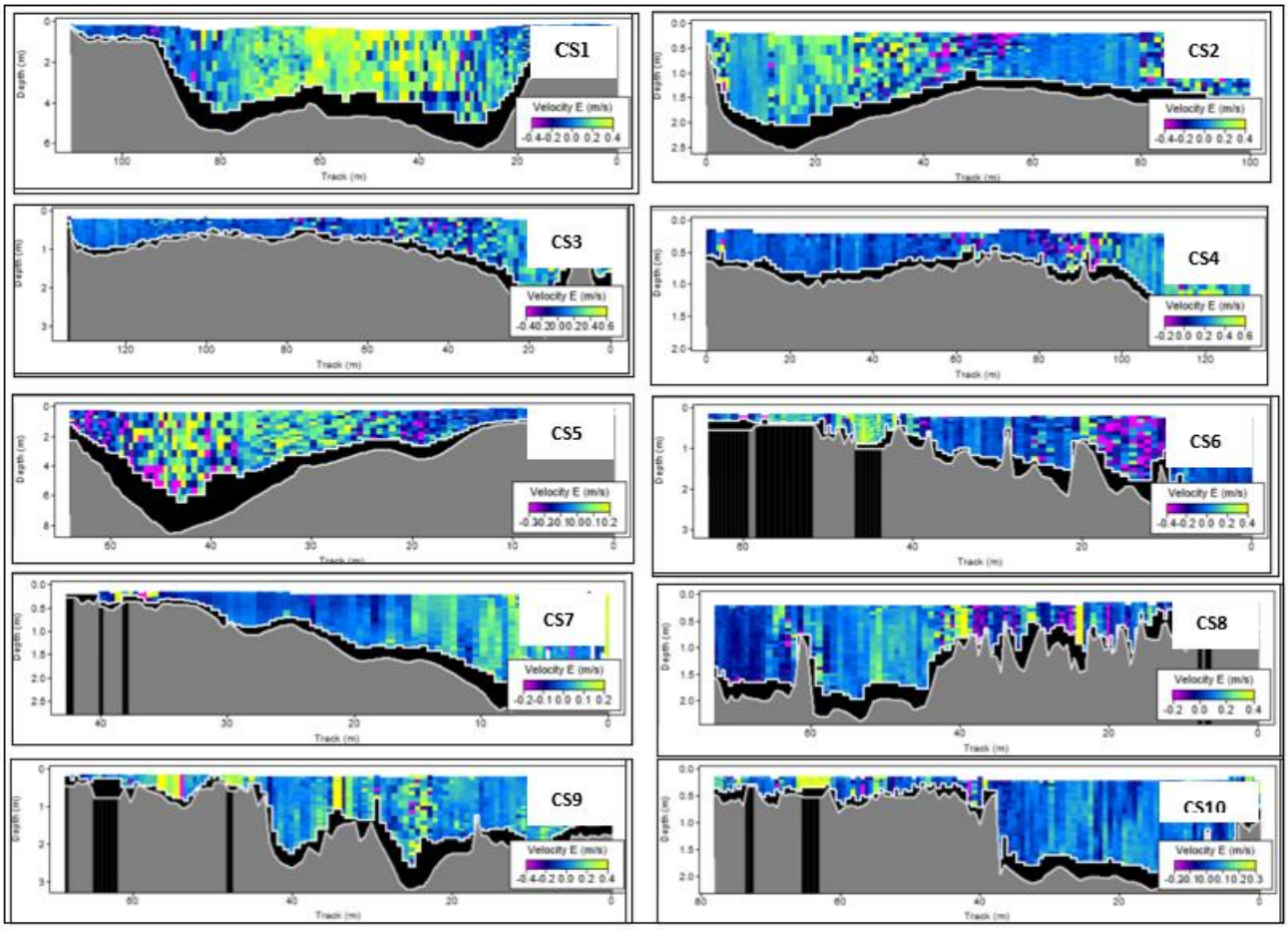

Figure 4. Cross-section profiles details

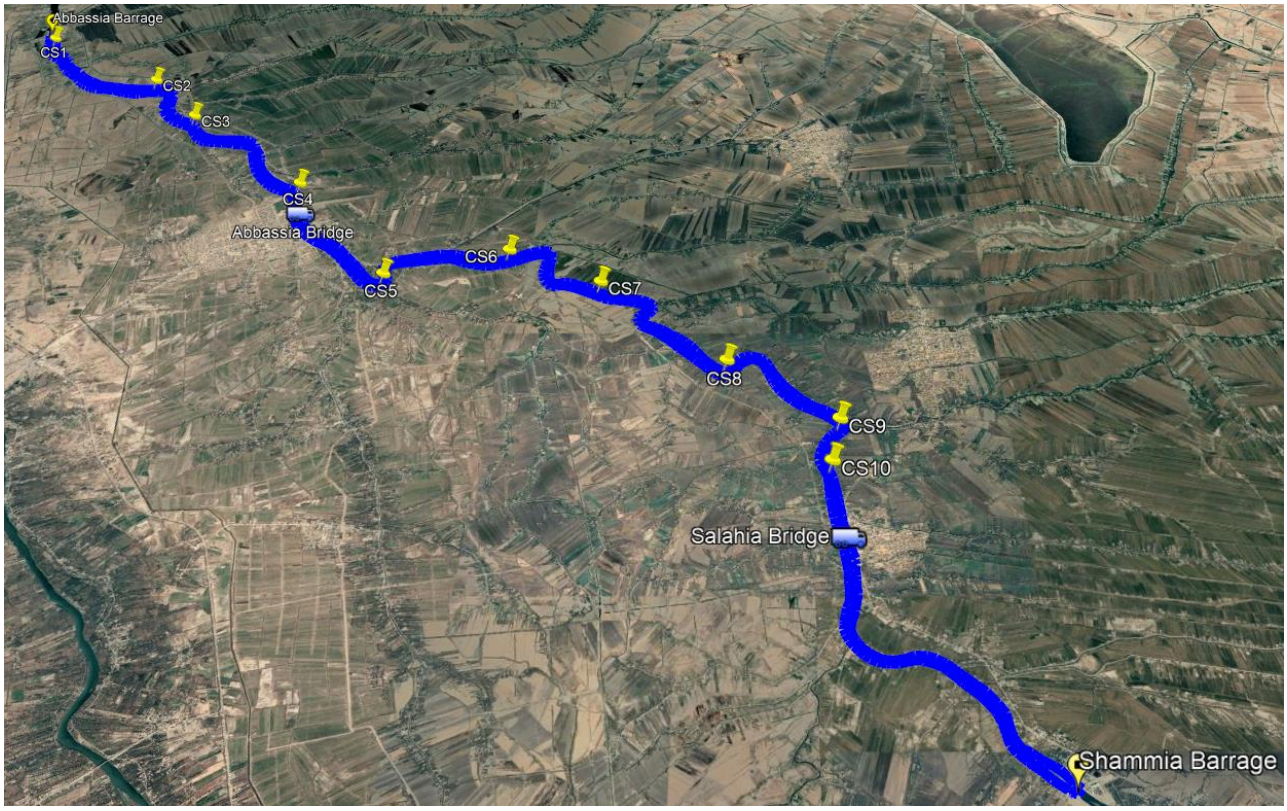

Figure 5. The cross-section's locations where the model is calibrated and validated

Figure 6. Field investigation through the study area

3. Results and discussion

As mentioned in the introduction, for comparison purposes, there is no similar work that has been conducted on the same area. Thus, the authors discussed the results below:

3.1. HECRAS2D hydraulic modeling software

The HECRAS2D software can simulate the unsteady flow in two-dimensional river systems. The equations employ the implicit finite volume solution approach. The implementation of the HECRAS2D-based model comprises the following steps: geometric preparation, creating a mesh, defining parameters, specifying

boundary conditions, calibrating, validating, and then using them in the sediment simulation process according to [19].

3.2. Geometrical preparation (terrain model)

A precise hydraulic model necessitates a comprehensive terrain model. Digital Elevation Models (DEMs) are essential elements in any modeling or numerical analysis that pertains to the topography and elevations of the Earth. USGS was used to obtain the DEM (digital elevation model) sentential 10m of the studied area [20]. Then, the file of the numerical model terrain was generated. Figure 7 illustrates the topography of the current investigation utilized in HECRAS2D.

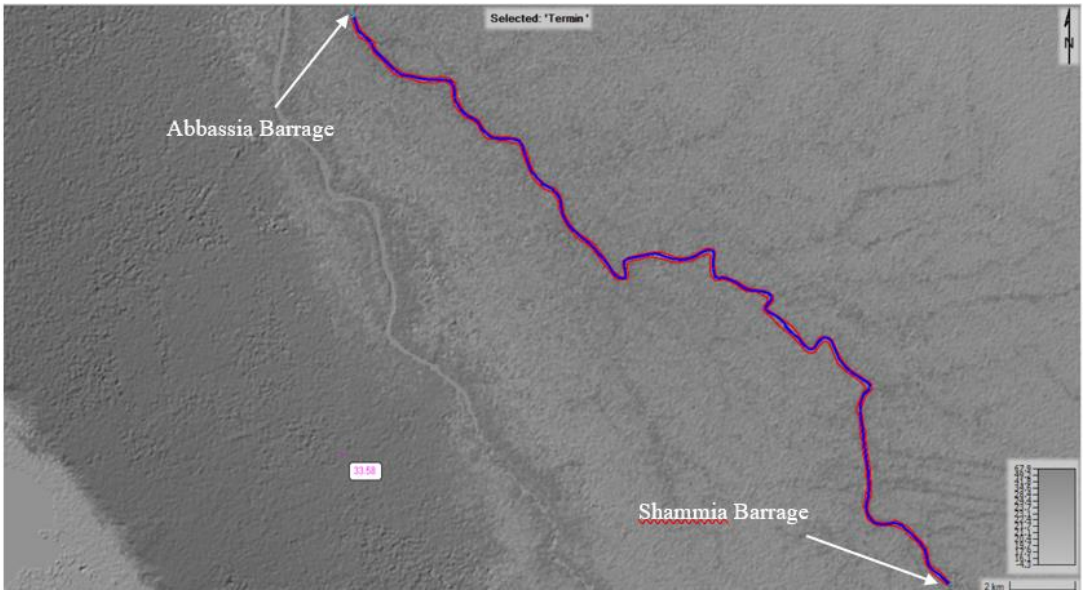

Figure 7. Digital elevation model for the study area [20]

3.3. Development of structured grid and time step

In numerical modeling, one of the essential procedures is developing an efficient grid. The results accuracy in 2D flow regions relies crucially on the computational time steps (ΔT) and careful selection of suitable sizes of mesh cells. In order to create an effective HEC-RAS computational mesh, the cell faces accurately must correspond to the highest point of flow barriers. In addition, suitable cell sizes should be selected in the designated area to represent the changing surface of water accurately as well as velocity [19]. Thus, the researchers evaluated the model with 20x20 mesh sizes in order for the most useful results to be determined (Figure 8). The model operated smoothly and flawlessly and showed excellent stability. In the HEC-RAS simulation, the duration of each calculation interval corresponds to the time step. The selection was determined by considering the dimensions of the grid and the velocity of the flow. By utilizing the fixed time step (fundamental approach), the computation time interval was predicted to be around 15 seconds.

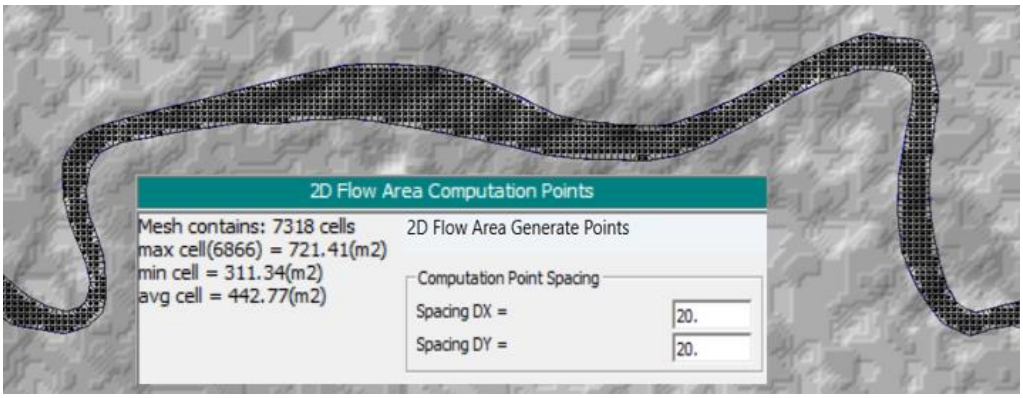

Figure 8. River mesh size (20x20) with 2D flow area computations characteristics

3.4. Boundary conditions and set of equations

One-year flow and stage hydrograph were developed spanning from January 1, 2023, to January 1, 2024. This data was used to determine the boundary conditions at the upstream and downstream locations. The selected data were designed to precisely reflect the hydraulic conditions of the flow area, in accordance with the calibration period for the recorded cross-sections. Various approaches can be employed to determine an energy gradient. Ultimately, the modeler must calculate an energy gradient. The energy gradient of 0.0001 for the Abbassia-Shammia section, as validated by [21], is obtained by computing the average slope of the stream. In HECRAS2D software there are two main equations, diffusion wave equation (DWE) and shallow water equation (SWE). It is crucial to recognize that the SWE option generally necessitates a shorter calculation interval than the diffusion wave strategy to ensure smooth and stable operation [19]. In this study, the model is configured with SWE without explicitly referencing any errors. The SWE postulates that the vertical length scale is significantly less than the horizontal scale. If the flow is assumed to be incompressible, the continuity equation can be represented by Equation 1:

$$\partial h/\partial t+(\partial(hu))/\partial x+(\partial(hv))/\partial y=q \quad (1)$$

where, t= time(T), h=water depth(L), u and v = velocity components in the x and y direction respectively, q=source/sink flux term.

3.5. Generation of land-cover data from satellite images

Manning's n value, which represents the coefficient of roughness, is commonly linked to land-cover classes in HEC-RAS 2D modeling for 2D flow regions. Estimating the roughness coefficient (n) in natural channels is challenging when doing field measurements. Multiple elements that influence the values of roughness coefficients [22]. The land cover classification data was obtained from the Esri website [23]. It was then imported into the RAS Mapper in HECRAS2D and linked with the terrain and geometrical file in the RAS Mapper. Manning's n values used for each land cover classification and their corresponding values in the National Land Cover Database (NLCD) are shown in Table 1.

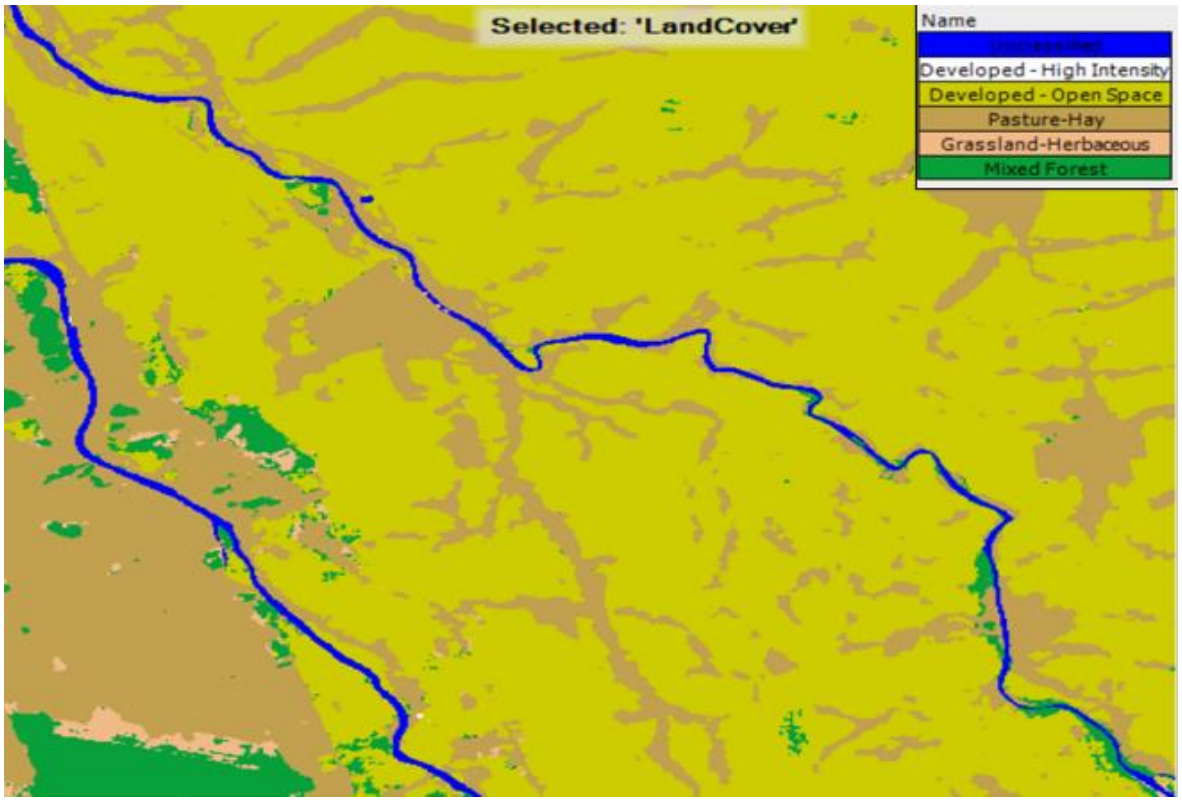

Figure 9. Region classification of land cover layer [19]

Table 1. Roughness coefficient for land covers classification of NLCD [19]

NLCD Value	Land Cover Definition	Range on n Value
11	Open Water	0.025-0.05
21	Developed, Open space	0.03-0.05
22	Developed, Low Intensity	0.08-0.12
24	Developed, High Intensity	0.12-0.2
43	Mixed Forest	0.1-0.16
71	Grassland/Herbaceous	0.07-0.16
81	Pasture/Hay	0.025-0.05

3.6. Calibration and validation of the hydraulic model

Calibration is the process of adjusting the parameter values of a model to correctly mimic the real-world response while adhering to specific performance standards that define an acceptable level of discrepancy between the model and reality [24], [25]. Based on the prior literature study conducted by [26] and [27], as well as [28], the Manning value was found to range between 0.03 and 0.04. The statistical markers R2 and RMSE were employed for calibration and validation, as outlined in the works of [29] and [30]. The current study utilizes data from ten cross-sections (CSs) for the aim of calibration, specifically to evaluate Manning's coefficient for the study reach. This is the process of evaluating the model's predicted accuracy by analyzing it with real data. This research considers the Manning roughness coefficient n values between 0.030 and 0.040. The model's estimated values of water surface elevation (WSE) at various values of n are compared to the observed water surface elevation recorded at ten cross-sections. The statistical indicator used for comparison is the root mean square error. The findings indicate that the utilization of the n = 0.04 values yields the highest level of concordance between the observed and calculated WSE, with an R2 value of 0.88 and an RMSE value of 1.19 (Figure 10).

The purpose of validation is to authenticate the results of the 2D unsteady flow model. Verification is a crucial undertaking in assessing the precision and variability of the model. Validation of 2D unsteady flow can be conducted by utilizing velocity data obtained from 10 measured cross-sections. Figure 11 presents a comparison conducted for the Abbassia-Shammia downstream reach, using a value of n = 0.04. The statistical indices, namely R^2 = 0.79 and RMSE = 0.048, indicate that the model outperformed in terms of velocity modeling. The benefit of the validation is to verify the results of the 2D unsteady flow model. Verification is an important task in analyzing the accuracy and uncertainty of the model. The validation of 2D unsteady flow can be performed using the flow velocity records for 10 CSs of measured cross-sections.

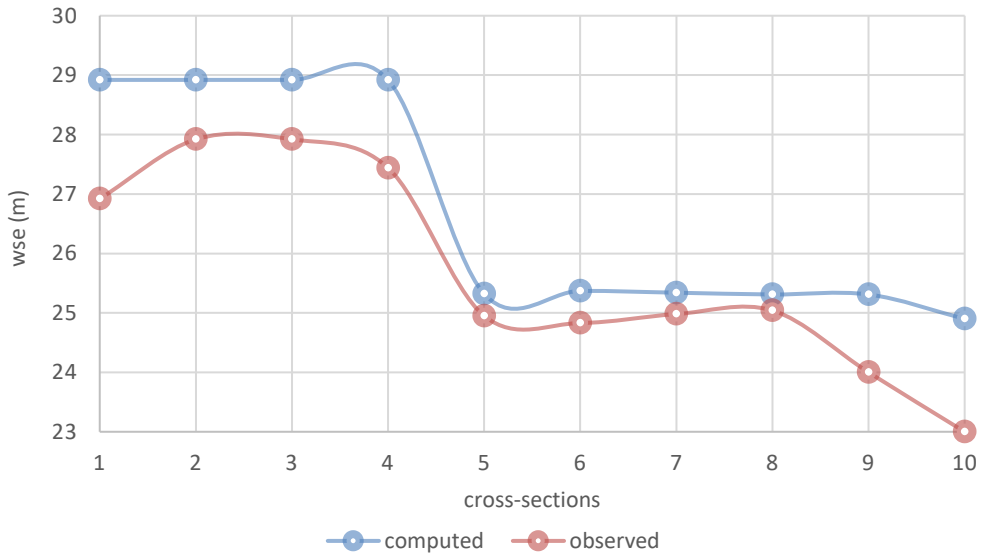

Figure 10. Measured vs. computed WSE along the river with 10 CSs (for calibration processes)

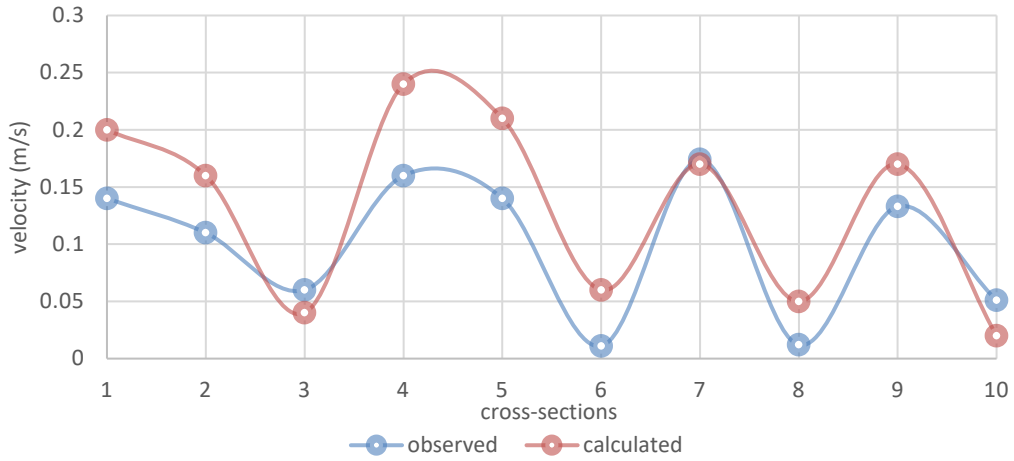

Figure 11. Observed vs. computed flow velocity with 10 CSs (for validation processes)

3.7. 2D sediment transport modeling

Following the calibration of the hydraulic model, sediment transport modeling was conducted. The model grid and Manning roughness values were obtained from a calibrated hydraulic model. The hydraulic simulation and sediment modeling used identical input data and settings. The input for the hydraulic model comprises the geometry of the system, grid dimensions, hydraulic boundary conditions, hydraulic equations, time intervals, current conditions, and Manning's roughness coefficient. Only the parameters and input relevant to the sediment modeling were changed. When comparing the results of the hydrodynamic model with the gradation of bed material and suspended load, it was found that only the WU sediment transport function, as described in the HECRAS2D user manual, aligned with the measurements taken in the studied area. The Soulsby fall velocity calculation technique formula and the active layer for sorting method are the most appropriate approaches for calculating the sediment transport characteristics in the specified section. For fall velocity calculations, this formula was derived by calibrating the aforementioned equations to the van Rijn sediment transport model and its definition for suspended sediment transport is as Equation 2 below:

$$q_{sk}^{*} = \begin{cases} 0.012Uh\left(\frac{U-U_{crk}}{\sqrt{R_k g d_k}}\right)^{2.4}\left(\frac{d_k}{h}\right) d_{*k}^{-0.6} & \text{for } U > U_{crk} \\ 0 \quad \text{otherwise} \end{cases} \qquad \text{.....} \qquad (2)$$

q_{sk}^{*} = fractional suspended-load sediment transport potential [L^2/T]
Rk = $\rho_{sk}/\rho_w - 1$ = submerged specific gravity of a particle [-]
Psk = sediment density [M/L^3]
ρw = water density [M/L^3]
U = effective depth-averaged current velocity [m/s]
Ucrk = critical depth-averaged velocity for incipient motion [m/s]

The formulas were initially suggested for sediments that are well-sorted. Here, the calculations have been adjusted for nonuniform sediments by substituting the median particle size with the diameter of the grain class and multiplying the critical depth-averaged current velocity by a correction factor that accounts for hiding and exposure. In this case, the concealing and exposure correction factor proposed by Wu et al. is employed. However, alternative factors could also be implemented.

3.8. Calibration and validation of sediment transport model

The model calibration approach included comparing the suspended load observed on March 21, 2023, and May 17, 2023, with the calculated suspended load at the identical cross-sections (10CSs) using the HECRAS2d model. To achieve this objective, the values of physical and numerical parameters stated Figure 12 were used to carry out this procedure. The calibration procedure of the hydrodynamic model yielded the following

performance metrics: R2 = 0.751. The statistical indicators demonstrate a strong and good correlation between the measured and estimated suspended load. The observed suspended load data exhibited a fluctuation with cross-sections, with values ranging from 134 mg/l at CS1, to 152 mg/l at CS4, and finally reaching 57 mg/l at the last cross-section. The presence of the concentration along the river may stem from either mineral or organic sources. Suspended particles also serve as sites of attachment for additional contaminants, such as metals and microorganisms. Typically, the total suspended levels rise throughout winter and decline during summer.

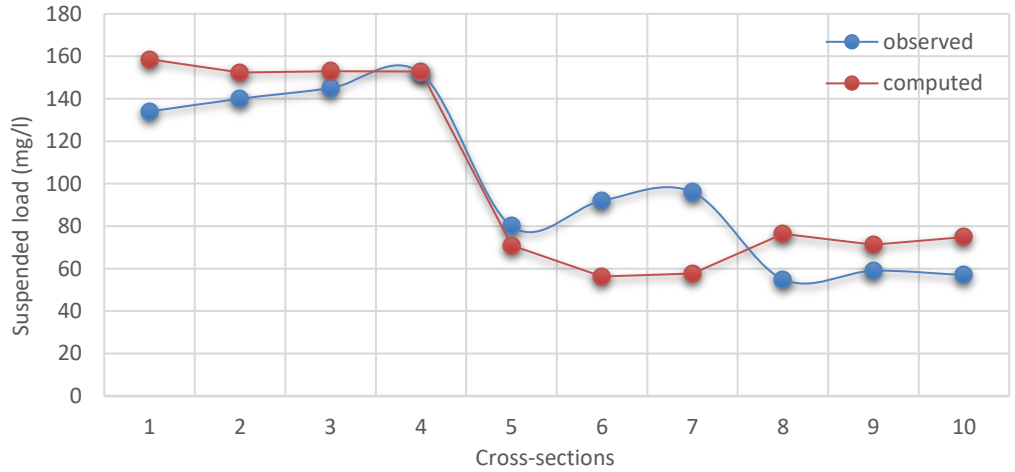

Figure 12. Measured vs. computed suspended load for ten CSs based on Calibration of HECRAS2D Model

The water surface elevation-based validity assessment demonstrates a strong correlation between the observed and calculated velocity, with R2 = 0.8751. Therefore, the outcomes of the validation procedure for the sediment transport model were deemed to be good and satisfactory (Figure 13).

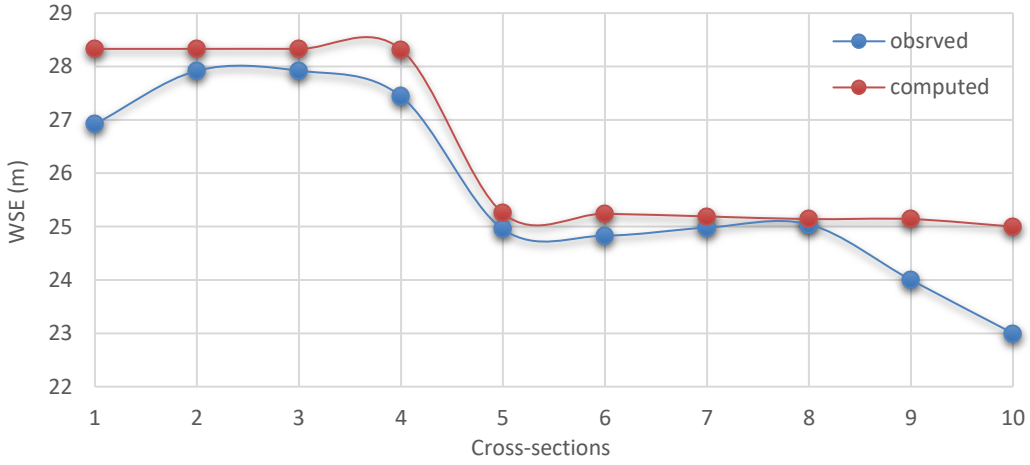

Figure 13. Measured vs. computed water surface elevation for ten CSs (WSE-based validity of HECRAS2D Model)

3.9. Sediment transport capacity (STC)

In addition to the trapping of sediment by the reservoir, another significant factor contributing to morphological changes downstream of hydraulic structures such as barrages is the considerable decrease in the capacity of water flow to carry sediment. The highest computed sediment transport capacity for the recorded flow and stage hydrograph in the study reach is 129.9 kg/m/s, occurring at a CS1 at a distance of 200 m from the Abbassia barrage and CS4 which is located near Abbassia Bridge. In this particular flow scenario, the low STC mostly spreads along (CS3, CS5) which represents before and after Abbassia Bridge and certain reach sections towards the downstream area (CS6, CS7, CS8, CS9, CS10) it means that the regions of the river near the upstream of study area had a high capacity of sediment transported comparable to downstream.

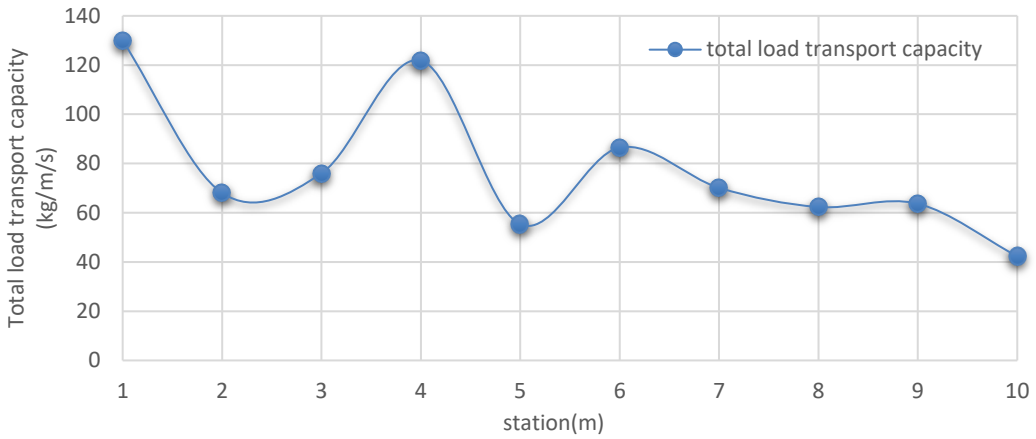

Figure 14. Shows sediment transport capacity according to the measured cross-sections

3.10. Sediment transport concentration

The study used the HEC-RAS2D model to examine the maximum grain size that can be carried by the river during the flow hydrograph. Additionally, it aimed to determine the lowest grain size that can be transported in the river reach, specifically focusing on the clay class. Figure 15 contrasts an aerial view of a comparable incident with the concentration outcome of the HEC-RAS 2D Abbassia-Shammia model. The model accurately replicates the total concentration pattern and flow field for the first 600 m distance of the river. Figure 16 demonstrates that the grain size gradation class that may be carried out most effectively according to measured cross-sections is the one consisting of clay, very fine silt (VFM), and very fine sand (VFS). Table 2 shows the default grain class diameter in (mm) [19].

Table 2. Default grain classes in HEC-RAS (mm)

Grain classes	Abbreviation	Lower bound (D, mm)	Upper bound (D, mm)	Mean diameter (D, mm)
Clay	Clay	0.002	0.004	0.003
Very fine silt	VFM	0.004	0.008	0.006
Very fine sand	VFS	0.0625	0.125	0.088

The sediment transport concentration (as suspended sediment) is defined according to the grain diameters. VFM ranges from 1399 to 295 mg/l, while the clay class ranges from 2115 to 295 mg/l. Nevertheless, the overall transport concentration varied from 1 to 3524 to 752 mg/l along the whole stretch (high value in yellow). For all classes, the first four cross-sections located upstream of the study area were the highest recorded value of sediment transported concentration then started to decrease towards the downstream studied reach.

Figure 15. Shows total sediment transport concentration at starting 600m river reach before (left) and after simulation (right)

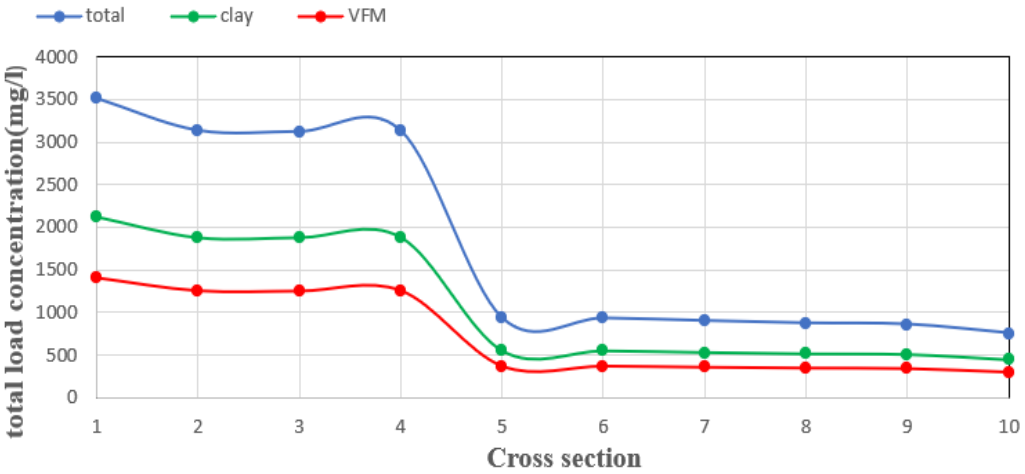

Figure 16. Shows sediment transport capacity along river reach

3.11. River bed change investigation

The HECRAS2D Model was used to analyze the properties of sediment transport and assess changes in the river bed during the course of the research. In order to achieve this objective, the flow hydrograph that occurred throughout the research period was examined. The outcome of this situation is shown in Figure 17, showing the river bed change when using a one-year flow hydrograph.

During a flow hydrograph, the river bed experiences variations between erosion (red regions) and deposition (blue regions). At the first stations from the Abbassia barrage, sedimentation in the river bed occurs by the sediment transported from the region before the barrage. After that, the river would fluctuate between erosion at narrow river cross-sections (that had high velocities) to sedimentation at wide river cross-sections (that had low velocities, islands presence, and where there were the vegetated regions). The erosion was increased towards the downstream area and it is a normal process at alluvial rivers.

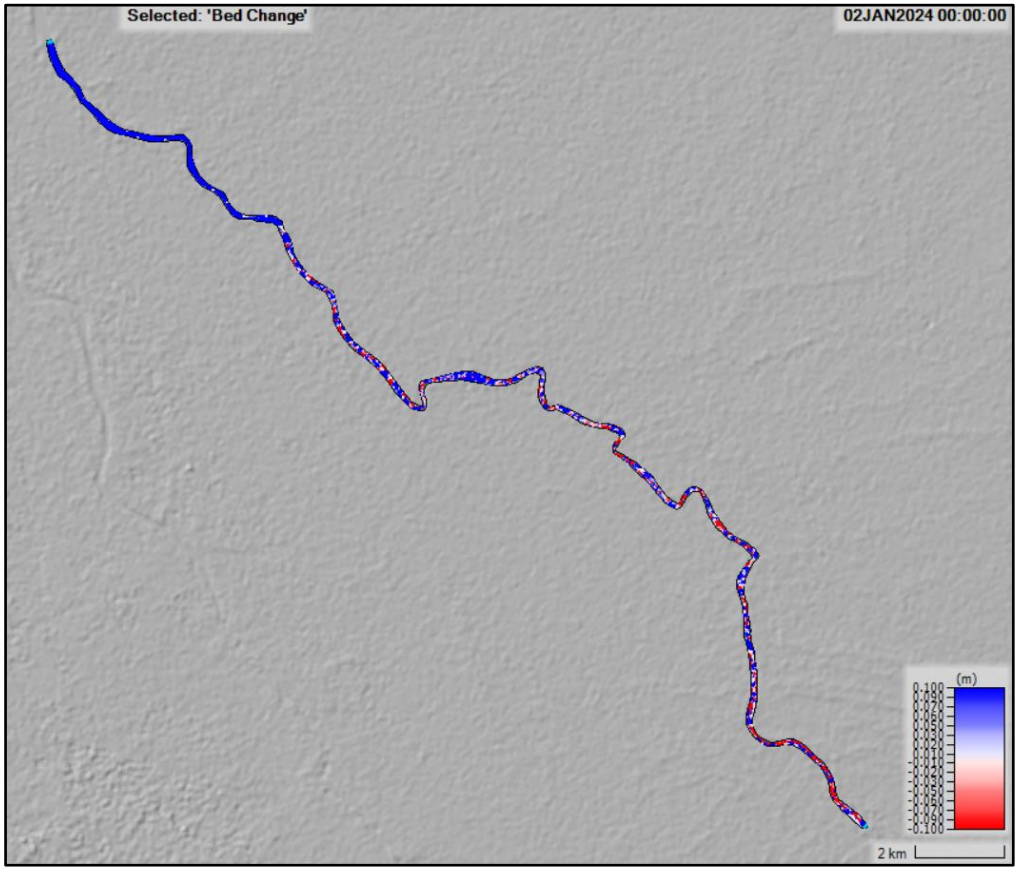

Figure 17. River bed change with one-year flow hydrograph

The value of bed change along the reach illustrated in Figure 18 shows that this value ranges between -5.72m to 5.87m. The deposition occurs along 69% of the reach. Most of the deposited reach length extended between stations 0 to 12000 m, with deposition depth of 5.78m max, 14000m to16000m, with deposition depth not exceeding 2.656m, and 23000m to 32000m, with deposition depth of no more than 3.71m. On the other hand, most of the eroded reach length extended between stations 8000m to 13000m, with an erosion depth of 1.8 m max. However, the reach part between stations 15000 and 32000m eroded with erosion depth not exceeding 5.72m.

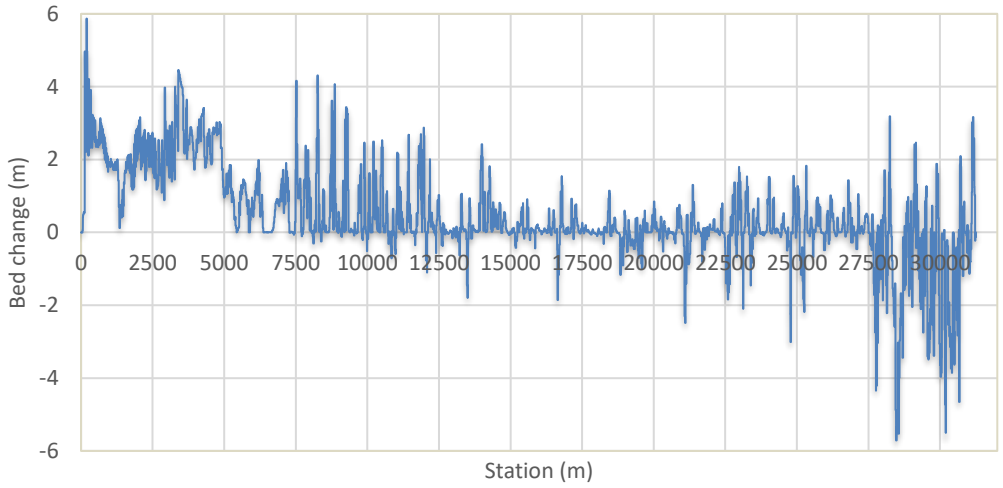

Figure 18. River bed change with one-year flow hydrograph 2023 along the river reach

4. Conclusions

This work investigates morphological behaviors of the Euphrates near Abbassia-Shammia reach considering the field study with available data that was requested officially from IMoWR, a one-year flow hydrograph as a boundary condition was used. The HECRAS2D model coupled with the field works was run, and the results were plotted. According to the results of this study, the most important conclusions are:

1. Using the Abbassia and Shammia barrages on the Euphrates, it is demonstrated that the upstream and downstream interactions of successive barrages interconnect to generate a unique morphological behavior for the river.
2. Calibration and validation processes were conducted, and the findings show that the value of Manning n=0.04, which indicates the closest agreement between measured and computed cross-sections for the reach under study.
3. Based on the inspection of the bed material samples, it has been determined that the predominant particle sizes observed within the designated river reach are fine sand and fine silt.
4. The highest computed sediment transport capacity for the recorded flow and stage hydrograph in the study reach is 129.9 kg/m/s, occurring at a CS1 at a distance of 200 m from the Abbassia barrage and CS4 which is located near Abbassia Bridge. In this particular flow scenario, the low STC mostly spreads along CS3 and CS5 which represents before and after Abbassia Bridge and a certain reach section towards the downstream area (CS6, CS7, CS8, CS9, CS10) it means that the regions of the river near the upstream of study area had a high capacity of sediment transported comparable to downstream.
5. The grain size gradation class that may be carried out most effectively according to the measured cross-sections is the one consisting of clay, very fine silt (VFM), and very fine sand (VFS). The sediment transport concentration for VFM ranges from 1399 to 295 mg/l, while for the clay class, it ranges from 2115 to 295 mg/l. However, the overall transport concentration varied from 1 to 3524 to 752 mg/l along the whole stretch (high value in yellow).

6. The bed change in erosion and sedimentation along the reach ranged between -5.72m to 5.87m respectively. The deposition occurred along 69% of the reach and most of the deposited reach length extended between station 0 to 12000m with deposition depth not exceeding 5.78m, 14000m to16000m with deposition depth of no more than 2.656m, and 23000m to 32000m with deposition depth not exceeding 3.71m. On the other hand, most of the eroded reach length extended between stations 8000m to 13000m with an erosion depth of 1.8m max. However, the reach part between stations 15000 and 32000m eroded with an erosion depth of no more than 5.72 m.

Author contribution

Conceptualization, Z.D.A. and J.S.M.; methodology, Z.D.A. and J.S.M.; software, Z.D.A.; validation, Z.D.A., and J.S.M.; formal analysis, Z.D.A.; investigation, Z.D.A. and J.S.M.; resources, Z.D.A.; data curation, Z.D.A.; writing—original draft preparation, Z.D.A.; writing—review and editing, J.S.M. and M.M.A; visualization, Z.D.A.; supervision J.S.M. and M.M.A.; funding acquisition, Z.D.A. All authors have read and agreed to the published version of the manuscript.

Declaration of competing interest

The authors declare that they have no known financial or non-financial competing interests in any material discussed in this paper.

Funding information

No funding was received from any financial organization to conduct this research.

References

[1] K. Fu and D. He, "Analysis and prediction of sediment trapping efficiencies of the reservoirs in the mainstream of the Lancang River," *Chinese Sci. Bull.*, vol. 52, no. Suppl 2, pp. 134–140, 2007.

[2] A. Singha and R. Balachandar, "Structure of wake of a sharp-edged bluff body in a shallow channel flow," *J. Fluids Struct.*, vol. 27, no. 2, pp. 233–249, 2011.

[3] W. Wang *et al.*, "Modelling hydrologic processes in the Mekong River Basin using a distributed model driven by satellite precipitation and rain gauge observations," *PLoS One*, vol. 11, no. 3, p. e0152229, 2016.

[4] V. J. Galay, "Causes of river bed degradation," *Water Resour. Res.*, vol. 19, no. 5, pp. 1057–1090, 1983.

[5] D. Stipić, L. Budinski, and J. Fabian, "Sediment transport and morphological changes in shallow flows modelled with the lattice Boltzmann method," *J. Hydrol.*, vol. 606, p. 127472, 2022.

[6] G. Di Silvio and M. Peviani, "Modelling short-and long-term evolution of mountain rivers: an application to the torrent Mallero (Italy)," in *Fluvial hydraulics of mountain regions*, Springer, 2005, pp. 293–315.

[7] G. Parker, "Selective sorting and abrasion of river gravel. I: Theory," *J. Hydraul. Eng.*, vol. 117, no. 2, pp. 131–147, 1991.

[8] A. Brenna, N. Surian, and L. Mao, "Alteration of gravel-bed river morphodynamics in response to multiple anthropogenic disturbances: Insights from the sediment-starved Parma River (northern Italy)," *Geomorphology*, vol. 389, p. 107845, 2021.

[9] J. S. Ribberink, *Mathematical modelling of one-dimensional morphological changes in rivers with non-uniform sediment*, no. 87. Citeseer, 1987.

[10] C. Ma, D. Qiu, X. Mu, and P. Gao, "Morphological Evolution Characteristics of River Cross-Sections in the Lower Weihe River and Their Response to Streamflow and Sediment Changes," *Water*, vol. 14, no. 21, p. 3419, 2022.

[11] W. Bertoldi, L. Zanoni, and M. Tubino, "Assessment of morphological changes induced by flow and

flood pulses in a gravel bed braided river: The Tagliamento River (Italy)," *Geomorphology*, vol. 114, no. 3, pp. 348–360, 2010.

[12] L. Mao and N. Surian, "Observations on sediment mobility in a large gravel-bed river," *Geomorphology*, vol. 114, no. 3, pp. 326–337, 2010.

[13] L. J. B. Eagle, J. L. Carrivick, A. M. Milner, L. E. Brown, and M. J. Klaar, "Repeated high flows drive morphological change in rivers in recently deglaciated catchments," *Earth Surf. Process. Landforms*, vol. 46, no. 7, pp. 1294–1310, 2021.

[14] N. Al-Ansari, N. Adamo, V. Sissakian, S. Knutsson, and J. Laue, "Water resources of the Tigris River catchment," *J. Earth Sci. Geotech. Eng.*, vol. 8, no. 3, pp. 21–42, 2018.

[15] K. R. Abed, M. H. Hobi, and A. J. Jihad, "Numerical modeling of sediment transport upstream of Al-Ghammas barrage," *Int. J. Sci. Eng. Res.*, vol. 5, no. 11, pp. 469–477, 2014.

[16] M. H. Hobi, "Analytical Study of Haditha Reservoir Sedimentation by CFD Model," *J. Babylon Univ. Sci.*, vol. 22, no. 2, p. 2014, 2014.

[17] M. S. Mahmood, K. R. Almurshedi, and Z. N. Hashim, "Non-linear regression models for hydraulic geometry relationships in Al-Abbasia meandering reach in Euphrates River," *Jordan J. Civ. Eng.*, vol. 11, no. 4, 2017.

[18] "Ministry of Water Resources, General Authority for Dams and Reservoirs Dams, Directorate Najaf Branch, unpublished data, 2022" Accessed: Jun. 07, 2024. [Online]. Available: https://mowr.gov.iq/

[19] "HECRAS2D User Manual**,** Version 6.3**,** Exported - May 2023." Accessed: Jun. 07, 2024. [Online]. Available: https://www.hec.usace.army.mil/confluence/rasdocs/r2dum/latest

[20] "USGS. Science for a Changing World. U. S. Department of Interior, Washington, United States. Available online: https://earthexplorer.usgs.gov/ (accessed on January 2023). " [Online]. Available: https://earthexplorer.usgs.gov.

[21] J. Homan and H. Toniolo, "Developing guidelines for two-dimensional model review and acceptance," University of Alaska Fairbanks. Center for Environmentally Sustainable …, 2018.

[22] V. T. Chow, "Open channel hydraulics. MacGraw-Hill Book Co," *Inc., New York, NY*, vol. 206, 1959.

[23] "No Title." [Online]. Available: httpp // Esri. Landcover classification

[24] J. C. Refsgaard and H. J. Henriksen, "Modelling guidelines—terminology and guiding principles," *Adv. Water Resour.*, vol. 27, no. 1, pp. 71–82, 2004.

[25] N. Kannan, C. Santhi, M. J. White, S. Mehan, J. G. Arnold, and P. W. Gassman, "Some challenges in hydrologic model calibration for large-scale studies: A case study of SWAT model application to Mississippi-Atchafalaya River Basin," *Hydrology*, vol. 6, no. 1, p. 17, 2019.

[26] L. K. Hameed and S. T. Ali, "Estimating of Manning's roughness coefficient for Hilla River through calibration using HEC-RAS model," *Jordan J. Civ. Eng.*, vol. 7, no. 1, pp. 44–53, 2013.

[27] L. K. Hameed and H. S. Mohammed, "Calibration of Manning's friction factor for rivers in Iraq using hydraulic model (Al-Kufa River as case study)," *Int. J. Innov. Sci. Eng. Technol.*, vol. 1, no. 10, pp. 504–515, 2014.

[28] A. S. Mustafa, S. O. Sulaiman, and K. M. Al_Alwani, "Application of HEC-RAS model to predict sediment transport for Euphrates River from Haditha to Heet 2016," *Al-Nahrain J. Eng. Sci.*, vol. 20, no. 3, pp. 570–577, 2017.

[29] H. Akay, B. Koçyiğit, and A. M. Yanmaz, "a case study for determination of hydrological parameters in HEC-HMS in computing direct runoff," in *12th International Congress on Advances in Civil Engineering (ACE) at Istanbul*, 2016.

[30] V. K. Pandey and R. K. Panda, "Calibration and validation of HEC-RAS model for minor command in coastal region," *Int J Curr Microbiol App Sci*, vol. 9, no. 2, pp. 664–678, 2020.

This page intentionally left blank